Top Catal (2014) 57:25–32
DOI 10.1007/s11244-013-0159-2

ORIGINAL PAPER

Electronic Structure Effects in Transition Metal Surface Chemistry

A. Vojvodic · J. K. Nørskov · F. Abild-Pedersen

Published online: 5 November 2013

Abstract Based on density functional theory and the Newns–Anderson model we present a detailed study of how an inclusion of higher order moments of the density of states can explain observed fine structure variations in oxygen bonding at metal surfaces. The many and sometimes closely coupled parameters that define the band-structure and its position are shown to force the very late transition metals to change shape abruptly. This induces variations in bond-strengths, which are not captured by the simple but successful d-band model. We demonstrate that these variations can be recaptured by a slight modification of the descriptor.

Keywords Newns–Anderson model · d-Band model · Electronic structure · DFT · Adsorption

1 Introduction

At the heart of surface chemistry phenomena is the understanding of breaking and formation of bonds at surfaces. Ever since the time of the pioneering work of Langmuir [1], the interaction of atoms and molecules with surfaces has been a vivid research area. In particular, the study of these elementary processes on transition metal surfaces was early realized and has been shown to form a foundation for our knowledge of surface reactions. Identification of the underlying features of these surface processes is key in almost every field within surface science, from materials science to catalysis.

In industry most important large-scale chemical processes are catalyzed by heterogeneous catalysts and many of the catalysts with the necessary properties are based on scarce materials such as Pt, Pd, Ru, and Rh. Therefore, finding non-precious alternatives is a problem of significant technological and scientific importance and vital for a sustainable energy future of our society. The search for these potential catalysts can be made possible and speeded up significantly if a deeper knowledge of the individual elementary surface processes exists.

Solid surfaces applied as catalysts are optimized based on their ability to adsorb reactants, break specific bonds, form new ones between intermediates in close proximity, and finally desorb the products formed. This has shown to involve a study of material specific electronic features and in particular the behavior of metal electronic d-states at the surface of transition metal based catalysts. Over the years, a lot of effort has been made to elucidate the role that the d-electrons play for chemisorption and catalysis. They have been anticipated [2], estimated [3], and articulated in the so-called d-hybridization picture, which over the last decade has shown tremendous successes in describing the interaction between a metal and an adsorbate state [4–18]. In this picture an approximate quantitative measure can be set up in which the additional hybridization induced between the metal d-states and the adsorbate state can be explained. For metal systems including pure transition metal surfaces, alloys with homogeneous overlayers, alloys with heterogeneous surface layers, surfaces with steps and strains, and surfaces with poisons and promoters (see [7–14]), the model has had a great success. However, there are

A. Vojvodic · J. K. Nørskov · F. Abild-Pedersen (✉)
Center for Interface Science and Catalysis, SLAC National Accelerator Laboratory, 2575 Sand Hill Road, Menlo Park, CA 94025, USA
e-mail: abild@slac.stanford.edu

A. Vojvodic · J. K. Nørskov
Department of Chemical Engineering, Stanford University, Stanford, CA 94305, USA

a few cases where the model has been shown to be inadequate [19, 20].

In the following paper, we challenge the simple d-band model by a direct comparison with the more detailed tight-binding model, the so-called Newns–Anderson (NA) model. We discuss the regimes where the d-band model is valid and applicable. Finally, we introduce an alternative descriptor, which is able to capture the fine structure effects that we observe. We will first give a very short summary of the two models that form the basis of this paper. This will be followed by a presentation of our results and a discussion.

2 Brief on Chemisorption Models for Transition Metals

Adsorption on a surface occurs when an atom or a molecule (adsorbate) is bound in the vicinity of the surface. Depending on the strength of this bond a sharing of adsorbate and surface electrons will be involved and the energy levels of the adsorbate will be perturbed (the perturbation of the surface states due to the presence of the adsorbate is in most cases negligible [21]). The strength of adsorbate–surface bonds can be estimated from the NA model [2, 22]. According to the NA picture, when the adsorbate approaches the surface the one-electron states on the adsorbate begin to interact with all the valence surface states. The overlapping surface states form an almost continuous band of states and the strength of the interaction depends on the shape of these bands. If the surface associated band is broad, i.e. delocalized in energy space, the interaction will result in a broadened single adsorbate localized resonance, with energy lower than the original gas phase adsorbate level. If, on the other hand, the surface associated band is narrow, i.e. localized in energy space, the adsorbate state will split into bonding and anti-bonding resonances, with energies above and below the original gas phase adsorbate level, respectively [23].

Adsorption on transition metal surfaces provides a scenario were both interaction types are present that is, the adsorbate level interacts both with a broad s-band and a narrow d-band. Assuming that the overall adsorbate–surface interaction is separable, the adsorption energy is

$$\Delta E_{\mathrm{ads}} = \Delta E_0 + \Delta E_{\mathrm{d-hyb.}}. \quad (1)$$

As described, the interaction between a single adsorbate state and the s-states will give rise to a broadened adsorbate single resonance state (renormalized state). Since all transition metals have similar half-filled broad s-bands, the energy associated with this interaction ΔE_0 can be assumed to have a constant contribution for all metals. Hence, the adsorption energy difference from one metal to the next will be determined by the interaction of the single renormalized resonance with the metal d-states, denoted by $\Delta E_{\mathrm{d\text{-}hyb}}$. When the coupling strength between the renormalized state and the d-states is weak, then to a first approximation, variations in the binding energy should only depend on the position of the d-states relative to the Fermi [21, 24, 25]. This in essence describes the d-band model [25].

Through the NA approach one can estimate the contribution from the interaction between the renormalized adsorbate state and the d-states for each transition metal. In the following, we show to what extent this approach is possible, by comparing features of the electronic structure obtained from density functional theory (DFT) calculations with information obtained from the analytical NA model. We focus on the most close-packed surfaces of the 3d–5d transition metals in their ground-state structure.

3 Results and Discussion

The interaction between the large number of d-electronic states at the metal surface forms a well-defined band-structure. This can be mapped out by studying the density of d-states projected onto a single surface metal atom. Clearly, due to the intricate nature of the interaction we expect the density of states (DOSs) to have a distribution with a complex and detailed structure as a function of energy. Nevertheless, we shall use a much simpler functional form, that of a semi-ellipse, for the DOS distribution and show that the hybridization energies obtained agree well with the energies related to the real distributions, here taken as the DOS obtained from DFT calculations.

The hybridization energy due to the interaction between an adsorbate energy level, of degeneracy n_{a} and with energy ε_{a}, and the distribution of energy levels at the surface is given by: [26]

$$\Delta E_{\mathrm{d-hyb.}} = \frac{2}{\pi}\int_{-\infty}^{0} \mathrm{Arc\ tan}\left(\frac{\Delta(\varepsilon)}{\varepsilon - \varepsilon_{\mathrm{a}} - \Lambda(\varepsilon)}\right)\mathrm{d}\varepsilon - n_{\mathrm{a}}\varepsilon_{\mathrm{a}}, \quad (2)$$

where $\Delta(\varepsilon) = \sum_k |V_{\mathrm{ak}}|^2 \delta(\varepsilon - \varepsilon_k)$ and its transform $\Lambda(\varepsilon) = \frac{1}{\pi} P \int_{-\infty}^{\infty} \frac{\Delta(\varepsilon')}{(\varepsilon - \varepsilon')} \mathrm{d}\varepsilon'$ represent the adsorbate-induced changes to the metal states times the coupling between the adsorbate and the metal states. In the expression for the transform, P is the principal value of the integral. To be noted is that Eq. 2 can be applied to any DOS distribution to get the interaction energy between that particular distribution and an adsorbate level.

Since the adsorbate induced changes in the DOS of the metal can be considered an insignificant perturbation compared to the metal induced changes on the adsorbate state. We shall assume in the following that the d-projected DOS is a reasonable approximation of $\Delta(\varepsilon)$.

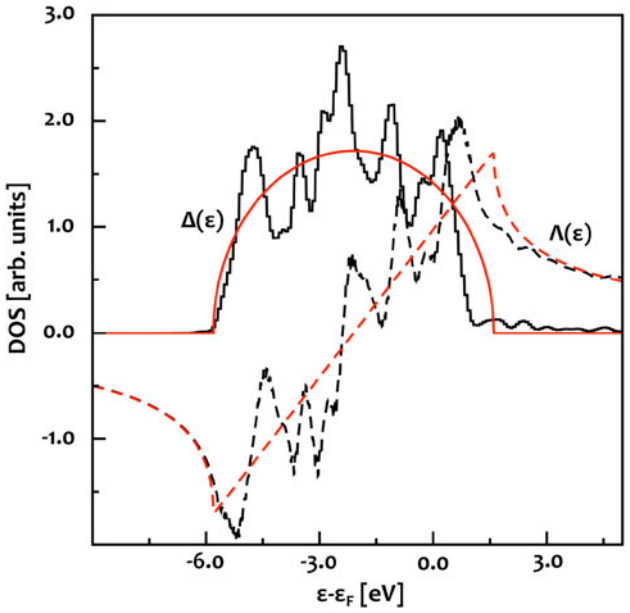

Fig. 1 Calculated metal projected d-states $\Delta(\varepsilon)$ (*solid*) and the corresponding mathematical transform $\Lambda(\varepsilon)$ (*dashed*) for the Rh(111) surface. The *black lines* represent data extracted from the DFT calculation and the *red lines* show the results obtained for the semi-elliptical fit to the DFT calculation

In Fig. 1, we show the DOS distribution of d-states projected onto a single metal atom in the surface layer of Rh(111) as obtained from DFT calculations and the semi-elliptic fit to this distribution. Here, the Rh(111) surface serves as a representative example for the other close-packed transition metal surfaces. The semi-elliptic fit was obtained by conserving both the center of the distribution and the filling, which is given by the number of states below the Fermi level, where $\varepsilon_F = 0$. The mathematical transforms $\Lambda(\varepsilon)$ for the two distributions are also shown in Fig. 1 as dashed lines. The DFT DOS exhibits a rich structure, which is inherited by $\Lambda(\varepsilon)$. This relation between $\Delta(\varepsilon)$ and $\Lambda(\varepsilon)$ is also evident for the semi-elliptic fitted distribution and it shows a much smoother behavior.

Table 1 summarizes the values needed to represent the electronic properties and coupling strengths of the different metals. The first moment, ε_d, of the electronic density of state distribution $\rho(x)$ and the nth moment, m_n^c, of $\rho(x)$ centered at ε_d are defined as

$$\varepsilon_d = \frac{\int_{-\infty}^{\infty} x\rho(x)\mathrm{d}x}{\int_{-\infty}^{\infty} \rho(x)\mathrm{d}x}, \tag{3}$$

and

$$m_n^c = \frac{\int_{-\infty}^{\infty} (x-\varepsilon_d)^n \rho(x)\mathrm{d}x}{\int_{-\infty}^{\infty} \rho(x)\mathrm{d}x}. \tag{4}$$

The coupling strength between an adsorbate state and the metal d-states (see Table 1) depends on the adsorbate–metal coordination and the distance between the adsorbate and the metal surface [21]. However, it can be shown that variations in the matrix element V_{ak}, mainly depend on the spatial extent of the metal d-states, which can be defined by the electronic band-width and the element radius as

$$V_{ak}^2 = \eta \frac{M_a M_d}{r^{l_a+l_d+1}}. \tag{5}$$

Here η is given by structure constants in LMTO, l_i ($i = a, d$) is the angular momentum quantum number of adsorbate and metal, and $M_l = (s^{2l_i+1}\Delta_{l_i})^{1/2}$ where s is the neutral sphere radius and Δ_{l_i} is an LMTO potential parameter corresponding to the band-width. For a given adsorbate the relative coupling strengths in Table 1 are given by $\frac{V_{ak}^2}{V_{aCu}^2} = \frac{M_M}{M_{Cu}} \left(\frac{r^{l_{Cu}}}{r^{l_M}}\right)^2$.

A common assumption is that the adsorbate–surface bond lengths are similar. Hence, to lowest order approximation in bond length, the coupling matrix elements can be

Table 1 First moment (Eq. 3) and second moment (Eq. 4 with $n = 2$) of the semi-elliptical fits to the calculated DOS for a number of close-packed transition metal surfaces are shown in column one and two, respectively

Metal surfaces	ε_d (eV)	$m_{n=2}^c$ (eV)^2	$V_{ak}^2 = \left(\frac{V_{ak}^M}{V_{ak}^{Cu}}\right)^2$
Sc(0001)	1.18	2.19	7.90
Ti(0001)	0.70	3.05	4.65
V(110)	0.38	3.77	3.15
Cr(110)	−0.35	3.85	2.35
Fe(110)	−0.84	2.39	1.59
Co(0001)	−1.50	2.32	1.34
Ni(111)	−1.59	1.39	1.16
Cu(111)	−2.46	0.84	1.00
Y(0001)	1.14	4.33	17.30
Zr(0001)	0.72	5.22	10.90
Nb(110)	0.10	5.64	7.73
Mo(110)	−0.90	5.36	6.62
Ru(0001)	−1.95	4.30	3.87
Rh(111)	−2.10	3.44	3.32
Pd(111)	−1.78	1.27	2.78
Ag(111)	−4.04	0.75	2.26
Hf(0001)	0.66	6.99	11.90
Ta(110)	0.29	8.32	9.05
W(110)	−0.77	8.71	7.72
Re(0001)	−1.58	8.18	6.04
Os(0001)	−2.23	6.21	5.13
Ir(111)	−2.95	4.97	4.45
Pt(111)	−2.42	2.65	3.90
Au(111)	−3.36	1.61	3.35

The second moment has been centered at ε_d to give the second central moment. The last column shows the coupling matrix elements between an adsorbate and the various transition metals relative to the one on Cu, adapted from [27]

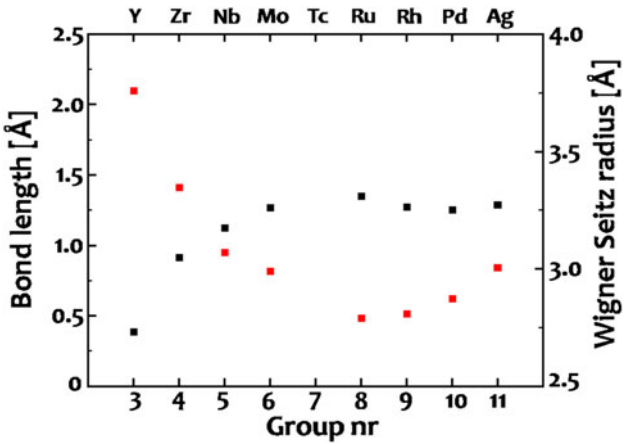

Fig. 2 Tabulated Wigner–Seitz radii (*red squares*) and perpendicular bond length between O and surface (*black squares*) as a function of the 4d metal group number. The bond lengths are obtained from DFT calculations were the surface atoms are fixed to their bulk positions and only the O is allowed to relax

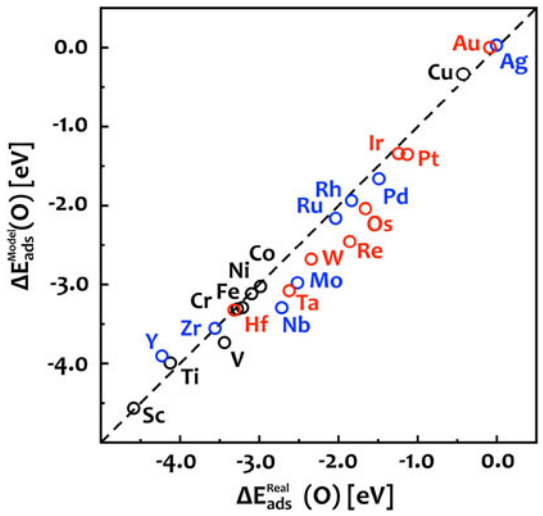

Fig. 3 Hybridization energies calculated using the Newns–Anderson model on the DFT-calculated (real) and the semi-elliptical (model) density of states. Coupling matrix elements are taken from Table 1 and the renormalized oxygen 2p adsorbate state is fixed at $\varepsilon_a = -5$ eV

estimated by bulk Wigner–Seitz radii and tabulated LMTO values for the widths of the bulk metal [27]. Figure 2 shows that the variation in Wigner–Seitz radii and the bond lengths are coupled and importantly that there is a significant difference between the early and the late transition metals. This implies that the simplified description based on Wigner–Seitz radii and bulk LMTO values is questionable for metals to the far left in the periodic table.

Before we proceed, it is instructive to introduce the simplified version of the interaction. If one assumes, that both the renormalized adsorbate state and the partially filled metal d-band can be approximated by single energy levels ε_a and ε_d, respectively, then the expression for the interaction becomes particularly simple [27].

$$\Delta E_{d-hyb.} = -\alpha \frac{V^2}{|\varepsilon_d - \varepsilon_a|} + \beta V^2, \tag{6}$$

α and β contain information about the filling of the d-states, the level degeneracy, and the spatial extent of the adsorbate level state. The first term is an attractive term given by the effect of hybridization between the adsorbate state and the d-states, whereas the second term is a repulsive term due to overlapping states. We note that the NA model only accounts for the attractive term in Eq. 6.

Given the distributions, the transforms, a fixed renormalized adsorbate energy level ε_a, and the coupling strengths between a metal level $|k|$ and the adsorbate level $|a|$, V_{ak}^2, we can now employ the NA model (Eq. 2) and estimate how well the semi-elliptic simplification of the DOS describes the hybridization energies compared to the real DOS distributions. This is shown in Fig. 3. We have assumed, that the coupling between an adsorbate state and metal d-states can be described by the values in the last column of Table 1. In addition, we have fixed the position of the renormalized state at -5 eV. This takes into account the estimated contribution from the interaction between an oxygen 2p state and the metal s electrons, which is $\Delta E_0 = 5$ eV, and makes up the largest contribution to the bond energy [21].

We find that the energies obtained using the simple semi-elliptical distribution as a model for the real DOS agree very well with the energies obtained using the real DOS distribution. The fact that we can use the semi-elliptical functional form for the DOS enables us to study trends in the hybridization energy in a controlled and mathematically well-defined way.

As can bee seen in Table 1, there are large variations in the coupling strength between the adsorbate and the d-states of the metal, which depend strongly on the metals position in the periodic table. Nevertheless, it has proven instructive to work in the coupling limit where $V_{ak} \ll |\varepsilon_d - \varepsilon_a|$. In this limit, assuming that ε_a is fixed, Eq. 5 leads to a linear scaling between variations in the binding energy with the position of the d-states to lowest order in ε_d.

By assuming a constant V_{ak}^2 in the semi-elliptical approach, here taken as $V_{ak}^2 = 1$, we are able to vary the center ε_d of the semi-elliptical distribution and the width W_d independently. The center is given by Eq. 3 whereas the mathematical expression for the width of a semi-elliptical distribution is given by $W_d = 4\sqrt{m_2^c}$. Using the NA model with $\varepsilon_a = -5$ eV we can now calculate the hybridization energy as a function of (W_d, ε_d).

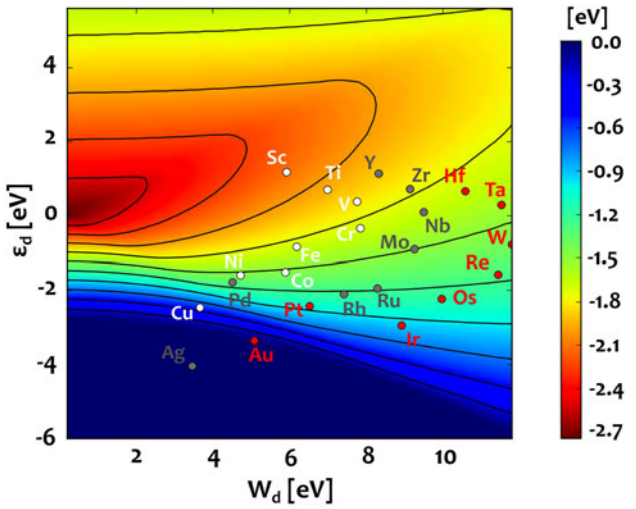

Fig. 4 Hybridization energies obtained with the NA model as a function of the center and width of the semi-elliptical representation of the density of states. Here the coupling matrix elements have been fixed at $V_{ak}^2 = 1$ and the renormalized state is kept at $\varepsilon_a = -5$ eV. The individual surface metal data points have been added to the plot based on the numbers from Table 1. Iso-energies are indicated with *black solid lines*

In Fig. 4, we show the calculated energy landscape using the NA model for $W_d \in [0; 12\text{ eV}]$ and $\varepsilon_d \in [-6; 5.5\text{ eV}]$. For a given width, as the center moves down relative to $\varepsilon_d = 0$, which corresponds to the Fermi level of the metal, the interaction energy decreases. In other words, as ε_d become more negative the band becomes more and more populated leading to a weaker interaction with the renormalized state. Furthermore, when the states are well below the Fermi level so that the d states are completely filled, the energy contribution becomes exactly zero. This corresponds to the coinage transition metals, which are known to have little or no attractive interaction between the adsorbate and their d-states. Another thing to notice is that the iso-energies lie very close and are almost parallel with the x axis just below the Fermi-level. This suggests, that transition metals in this region have bond-strengths that depend more strongly on variations in ε_d rather than on variations in W_d, which explains the success of the one-parameter Hammer–Nørskov d-band model for these elements. To illustrate the strength of this observation we have included the individual data points for all pure metals onto the landscape using the values ($W_d = 4\sqrt{m_2^c}$, ε_d) from Table 1. First, there is a clear distinction and ordering between the 3d, 4d, and 5d metals. Secondly, all pure late transition metals fall in the region with the parallel iso-energies, hence, the binding energies for these systems should show a pronounced scaling with the d-band center to lowest order. For the early transition metals, for example Sc, Y, and Zr, on the other hand, there is a clear deviation from this trend being positioned in the landscape where the iso-surfaces are both far apart and not parallel to the x axis. The exact transition between the "early" and "late" transition metals is a fine one and will be dependent on the adsorbate and in turn its interaction with the d-band states of the metal.

Figure 5a shows the relation between the W_d and ε_d values, for the semi-elliptical distribution for the 4d transition metal series, as extracted from Table 1. In the following, we will focus on the 4d metals but similar trends can be shown for 3d and 5d metals. For the late transition metals, Fig. 5a shows a clear trend where the width increases when the center of the distribution shifts up in energy. In the 4d series this is approximately linear, with Pd as an outlier. In fact, if one assumes such an approximate linear relation between the width and the center for these metals, and uses that the coupling strength is proportional to the width, one obtains that $V_{ak} \propto W_d \propto \varepsilon_d$. Hence, it follows immediately from Eq. 5 that the attractive term is proportional to ε_d. We also note that this approach should give rise to distinct lines for 3d–5d metals showing that only binding energies on late transition metals within a specific d-series should correlate with ε_d.

In Fig. 5b we show the binding energies of atomic oxygen on the most close-packed surfaces of the metals in the 4d series as obtained from DFT calculations as a function of the d-band center. A very good agreement between the binding energies and the d-band center is observed, again with Pd as a clear outlier. This suggests that the linear approximation between structure and position of the DOS distributions is valid and that the electronic deviations observed for Pd from that line are carried through to the DFT calculated binding energies. We also find that even the binding energies on the early transition metals seem to fall on the line shown in Fig. 5b. The reason is that as you move to the left in the periodic table the coupling between the metal states and the adsorbate increases. This has a large effect on the repulsion between overlapping states and hence these points are shifted to lower binding energies.

Figure 6a shows that there is an overall linear trend in the d-band center of the surface as a function of the group number of the metal and that the 3d–5d metals each form individual lines. However, Ni, Pd, and Pt are clear outliers to this trend. The separation between the 3d, 4d, and 5d metals is also evident in the d-band width of the surface, see Fig. 6b, that has a non-linear dependence on the group number. When it comes to the bulk, the bulk DFT DOS for each system has a lower lying d-band center and a wider d-band width as compared to the surface. In addition, the bulk DFT DOS shows the same trends as the surface DFT DOS including the outliers.

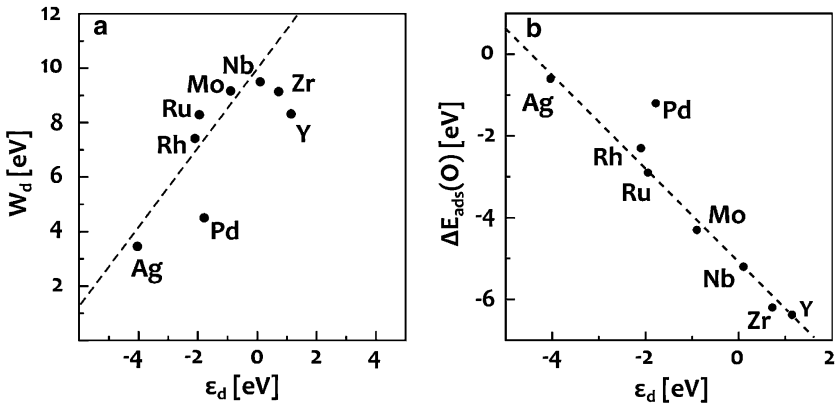

Fig. 5 **a** Variations in the semi-elliptical width of the density of states distribution as a function of the center of the distribution for the 4d series. **b** Calculated oxygen binding energies from DFT as a function of the center of the semi-elliptical DOS distribution

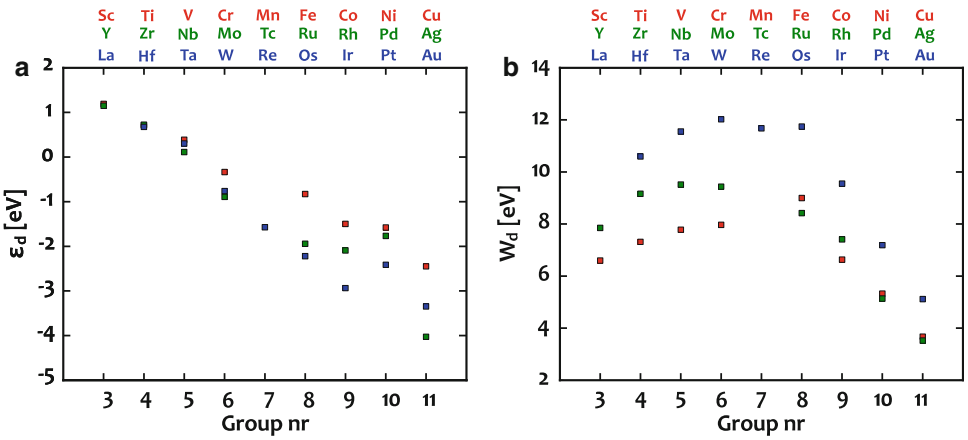

Fig. 6 Calculated d-band center (**a**) and width (**b**) for a metal atom in the first surface layer and the corresponding result for a metal atom based on DFT DOS

To elucidate the origin of the observed trends, we use a semi-elliptical model to calculate the d-band center. We assume an ideal d-band filling i.e. the filling is linear in the group number, and a second order polynomial dependence of the surface d-band width on the group number fitted to the $W_d = 4\sqrt{m_2^c}$ based on m_2^c values shown in Fig. 6b. The later assumption is rooted in the wave function overlap behavior. Figure 7a shows the predicted d-band center with a clear linear behavior from groups 3 to 9 and a non-linear trend for groups 10 and 11 i.e. Ni, Pd, Pt and Cu, Ag, Au, respectively, which should be compared to Fig. 6a. This clearly shows that the reason for Ni, Pt, and Pd being "outliers" from a linear trend, is a direct consequence of the d-band filling and the d-band width. The semi-elliptical model predicts that mathematically the coinage metals Cu, Ag, and Au, should have a higher d-band center than obtained from DFT and experiments. The reason we do not observe this, is that once the d-band is completely filled the position of the band is no longer pinned to the Fermi level and hence the d-band center can be shifted to lower energies to increase the stability of the system further. The same conclusions can be made (see Fig. 7b) combining the semi-elliptic model and assumptions with tabulated LMTO bulk metal widths (adapted from [28]).

Our findings show that the d-band center is a good descriptor for the O adsorption energy for metals if the d-band center and the d-band width show the same behavior as a function of group number and if the d-band is not almost or completely filled. Since the d states couple strongly in the NA picture to the renormalized adsorbate state giving rise to bonding adsorbate localized states below the d-band and anti-bonding adsorbate localized states above the d-band, one should utilize the information in the d-band width to define a refined descriptor for the binding energy. Figure 8 shows the d DOS of 4d transition metals. It is observed that the position of the upper-edge of the d-band is shifted down in energy as the position of the center of the DOS moves down. Such a behavior on its own would eliminate any dependence of the adsorption energy on the form of the DOS distribution. However, the mathematical relation between the position, form and filling forces the DOS to shift up in energy as the filling gets close to 1, as was demonstrated in Fig. 7. This explicitly breaks the correlation between the upper-edge position and the d-band center. As the bond strength is given by the position and filling of the anti-bonding states, which are pinned at the upper edge of the d-band, we suggest a refined energy descriptor, $\varepsilon_d^W = \varepsilon_d + W_d/2$. The introduction of a width

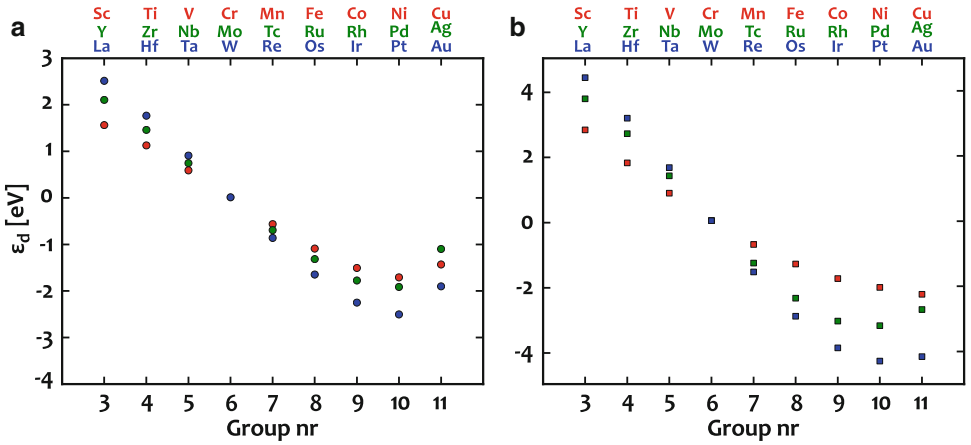

Fig. 7 **a** Approximated d-band center assuming a semi-elliptic shape of the d-band DOS. The assumptions are a linear dependence of the d-band filling on the group number, and a second order polynomial dependence of the width on the group number fitted to the semi-elliptic d-band widths given in Table 1. **b** Approximated d-band center assuming a linear dependence of the d-band filling on the group number, and a second order polynomial dependence of the width on the group number fitted to the LMTO bulk data adapted from [28]

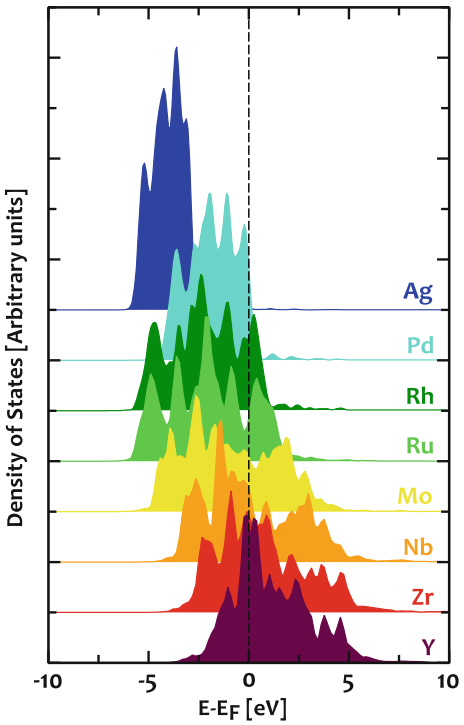

Fig. 8 DOS of the metal surface atoms for 4d metals as obtained from DFT calculations

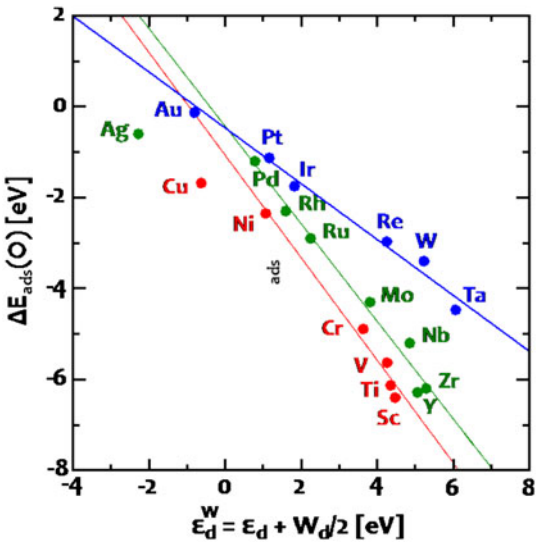

Fig. 9 The correlation between the DFT calculated O adsorption energies and the introduced electronic structure descriptor $\varepsilon_d^W = \varepsilon_d + W_d/2$ based on the DFT calculated DOS for metals. The linear regressions do not include Cu, Ag, and Au, respectively

dependence ensures correlation with the upper band-edge position and hence the bond strength. Figure 9 show the correlation between the DFT calculated O binding energy and the introduced descriptor. The new descriptor is able to capture the trends over the entire transition metal series. As expected the d metal with completely filled d band, Cu, Ag, and Au, for the 3d–5d metal series, respectively, have a non-linear dependence in ε_d^W as the position of the d-band is no longer pinned to the Fermi level. We note that our focus has been entirely on occupied states, however, for molecular adsorption the interaction between unoccupied renormalized states and the metal d-states will become important. Since the new parameter explicitly accounts for the structural changes of the d-band, we expect that the parameter should capture molecular adsorption strengths as well.

4 Conclusions

We have shown that basic reactivity trends of pure transition metals can be understood using the NA model on a

simple semi-elliptic approximation to the real DOSs. Plotting the obtained binding energies against the first and second-order moments of the density states indicates that binding on late transition metals vary stronger with the first moment for a group of transition metals thus substantiating the d-band model for which numerous examples both theoretical and experimental have shown to hold. The d-band model is a zero'th order approximation that describes how the bond strength varies as one moves through the periodic table. The model was originally introduced to study small variations in bond strength under perturbations of the electronic structure at the surface and has proven more than adequate for this [8, 14]. Having a simple electronic structure motif defining reactivity is crucial if one wants to take surface science and catalysis to the level of materials design. In the present paper we have extended the d-band model to explicitly take into account how the bond-strength depends on the depletion of the adsorbate anti-bonding state best defined through the upper-edge position of the d-states. The transition metals Ni, Pd, and Pt were identified to be most affected by the structure of the d-band and with the introduction of a generalized electronic structure descriptor, $\varepsilon_d + W_d/2$, one is able to correct for these effects explicitly.

Acknowledgments A. Vojvodic, J. K. Nørskov, and F. Abild-Pedersen gratefully acknowledge support from the U.S. Department of Energy, Office of Basic Energy Sciences.

References

1. Langmuir I (1961) In: Suits CG (ed) The collected works of Irving Langmuir. Pergamon Press Ltd., New York
2. Newns DM (1969) Phys Rev 178:1123
3. Lundqvist BI, Gunnarson O, Hjelmberg H, Nørskov JK (1979) Surf Sci 89:196
4. Gajdos M, Eichler A, Hafner J (2004) J Phys Condens Matter 16:1141
5. Hammer B (2006) Top Catal 37:3
6. Roudgar A, Gross A (2003) J Electroanal Chem 548:121
7. Greeley JP, Mavrikakis M (2004) Nat Mater 3:810
8. Kitchin JR, Nørskov JK, Barteau MA, Chen JC (2004) J Chem Phys 120:10240
9. Nikolla E, Schwank J, Linic S (2009) J Am Chem Soc 131:2747
10. Markovic NM, Ross PN (2002) Surf Sci Rep 45:121
11. Tripa CE, Zubkov TS, Yates JT, Mavrikakis M, Nørskov JK (1999) J Chem Phys 111:8651
12. Mills G, Gordon MS, Metiu H (2003) J Chem Phys 118:4198
13. Zhang JL, Vukmirovic MB, Sasaki K, Nilekar AU, Mavrikakis M, Adzic RR (2005) J Am Chem Soc 127:12480
14. Kibler LA, El-Aziz AM, Hoyer R, Kolb DM (2005) Angew Chem Int Ed 44:2080
15. Behm RJ (1998) Acta Phys Pol 93:259
16. Schnur S, Gross A (2010) Phys Rev B 81:033402
17. Menning CA, Chen JGG (2009) J Chem Phys 130:174709
18. Gross A (2008) J Comput Theor Nanosci 5:894
19. Liu ZP, Jenkins SJ, King DA (2004) J Am Chem Soc 126:10746
20. Inderwildi OR, Jenkins SJ, King DA (2007) Surf Sci 601:L103
21. Hammer B, Nørskov JK (2000) Adv Catal 45:71
22. Anderson PW (1961) Phys Rev 124:41
23. Holloway S, Lundqvist BI, Nørskov JK (1984) In: Proceedings of the 8th conference on catalysis, Berlin, vol IV, p 85
24. Hammer B, Nørskov JK (1995) Nature 376:2238
25. Hammer B, Nørskov JK (1995) Surf Sci 343:211
26. Bligaard T, Nørskov JK (2008) In: Nilsson A, Pettersson LGM, Nørskov JK (eds) Chapter 4 in "Chemical bonding at Surfaces and Interfaces". Elsevier, Amsterdam
27. Hammer B, Nørskov JK (1997) In: Lambert RM, Pacchioni G (eds) Chemisorption and reactivity on supported clusters and thin films. Kluwer Academic, Dordrecht, pp 285–351
28. Andersen OK, Jepsen O, Glötzel D (1985) Highlights in condensed matter theory, vol LXXXIX. Corso Soc. Italiana di Fisica, Bologna